Chandra ACIS Sub-pixel Resolution

D. -W. Kim[1], C. S. Anderson[1], A. E. Mossman[1], G .E. Allen[2], G. Fabbiano[1],
K. J. Glotfelty[1], M. Karovska[1], V. L. Kashyap[1], J. C. McDowell[1]

[1]Smithsonian Astrophysical Observatory,
[2]MIT Kavli Institute for Astrophysics and Space Research

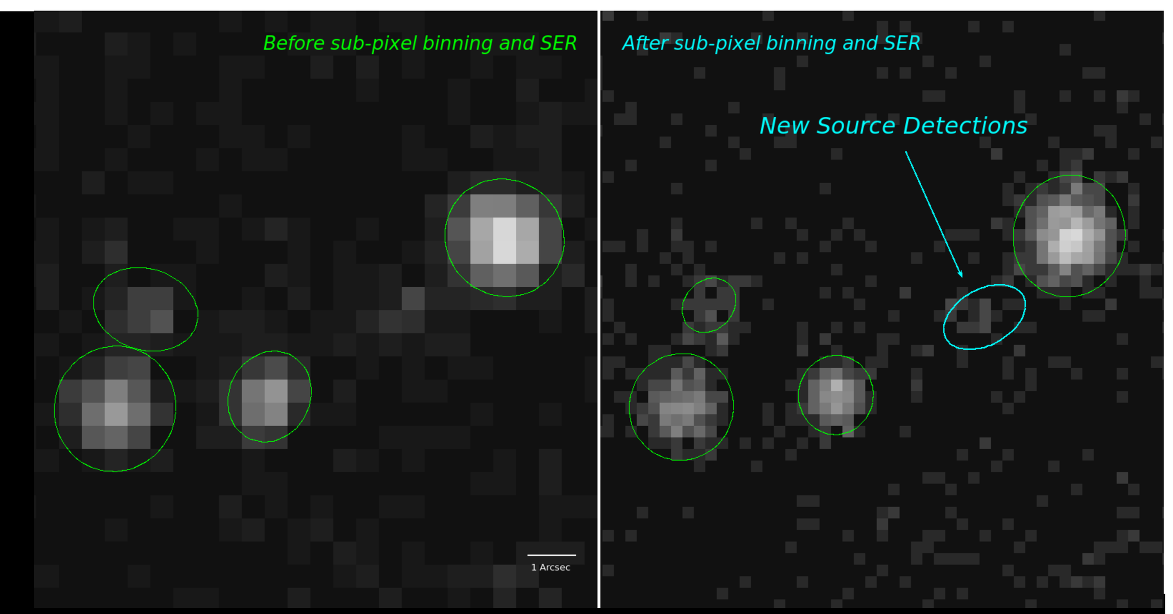

We investigate how to achieve the best possible ACIS spatial resolution by binning in ACIS sub-pixel and applying an event repositioning algorithm after removing pixel-randomization from the pipeline data. We quantitatively assess the improvement in spatial resolution by (1) measuring point source sizes and (2) detecting faint point sources. The size of a bright (but no pile-up), on-axis point source can be reduced by about 20-30%. With the improve resolution, we detect ~20% more faint sources when embedded on the extended, diffuse emission in a crowded field. We further discuss the false source rate of about 10% among the newly detected sources, using a few ultra-deep observations. We also find that the new algorithm does not introduce a grid structure by an aliasing effect for dithered observations and does not worsen the positional accuracy.

How to obtain the best possible resolution

1. Sub-pixel binning
Chandra coordinates (by dither + aspect correction) already contain positional accuracy finer than ACIS-pixel (0.492 arcsec).

2. Pixel-randonmization off
The current pipeline default is to apply pixel randomization by 1/2 ACIS pixel on the chip coordinate, to remove the instrumental "gridded" appearance of the data and to avoid any possible aliasing affects associated with this spatial grid.

3.ACIS sub-pixel algorithm
Improve position by fully utilizing 3x3 event islands
Implemented in CIAO 4.3 (acis_process_events)
For details, see http://cxc.harvard.edu/ciao/why/acissubpix.html

Previous algorithms:
Tsunemi, et al. 2001, Ap J, 554, 496 - first implementation
Mori, et al. 2001, in ASP Conf. Ser. 251, p576: Improvement by selecting the split pixel events
Li et al. 2003, ApJ, 590, 586 SER = subpix event repositioning
Li et al. 2004, ApJ, 610, 1204 EDSER = energy dependent subpix event repositioning

4. PSF deconvolution (not discussed here)

SN1987A
(Energy 300-5000eV)
Bin = 1 1/4 1/8

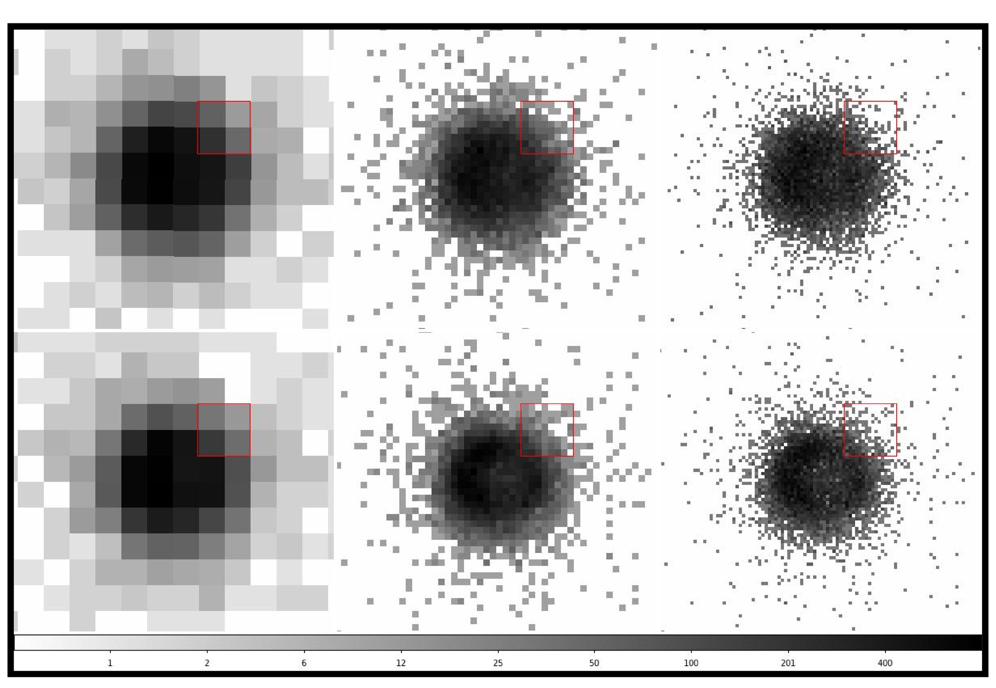

NGC 1386
(Energy 300-1000eV)
Bin = 1 1/4 1/8

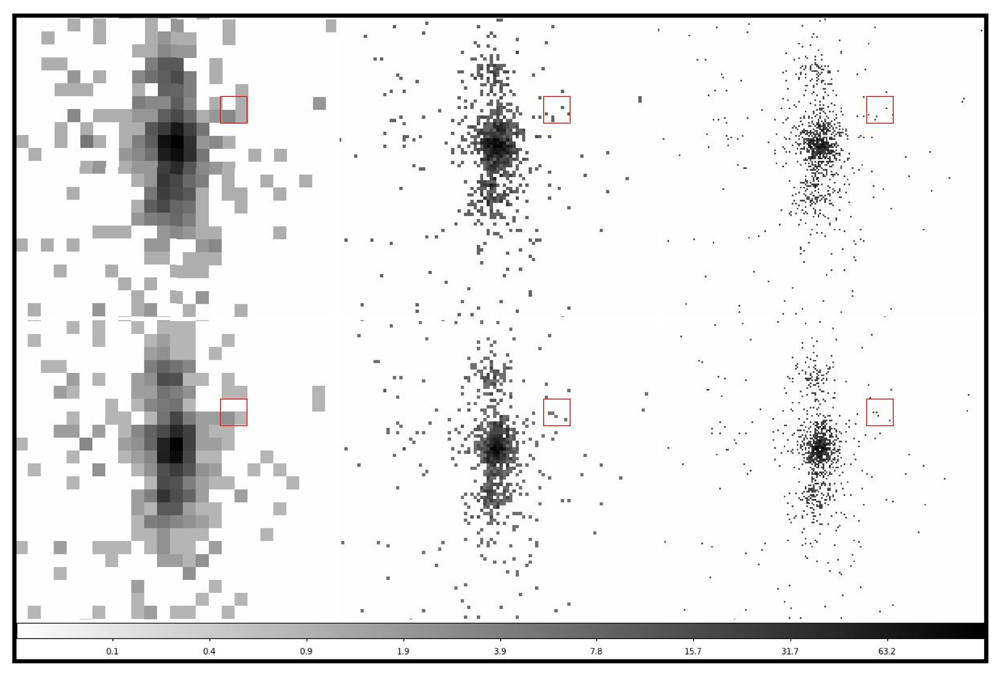

These examples illustrate the improved resolution for a bright extended source.

The top row contains the original image with bin 1, 1/4, and 1/8 pixel

These can be directly compared to the image below which uses the same bin parameter, but has pixel-randomization removed and a sub-pixel event repositioning algorithm applied.

(Red squares are 1 arcsecond per side.)

TEST 1: Improvement in point source sizes

Selected sample: Five bright, on-axis sources with pileup fraction less than 5%.
Two bright, off-axis sources with pileup fraction less than 5%.

obsid	ChaMP srcid	ra	dec	netB	off-axis angle (deg)	exp (sec)	cnt_rate (cnt/sec)	Pileup Fraction (%)
02228	XS02228B2_003	199.275644	29.154946	655	1.69	107754	0.006081	1
02254	XS02254B1_002	212.847632	52.225401	968	1.54	85638	0.011309	1
00927	XS00927B3_004	132.242264	44.909850	1255	0.59	121434	0.010336	1
01602	XS01602B7_005	96.504530	82.056729	533	0.40	41663	0.012800	2
03140	XS03140B7_001	178.935791	-1.794445	516	0.58	28010	0.018431	2
04964	XS04964B7_001	180.096222	55.527607	1436	5.83	66320	0.021664	3
04936	XS04936B7_011	163.320038	57.597492	2510	4.00	76227	0.032941	4

Source Size as measured by a CIAO tool, "srcextent" which calculates the size (sigma) and associated uncertainty of a photon-count source image using the Mexican Hat Optimization algorithm (Houck 2007).
The uncertainty (at 90% confidence) is derived from Monte Carlo trials.

	no binning			binning by 1/2 pixel			improvement(%)	
	a	b	c	A	B	C	a->A	a->C
02228	0.51 (0.47-0.54)	0.48 (0.44-0.53)	0.47 (0.43-0.52)	0.44 (0.40-0.47)	0.41 (0.38-0.44)	0.40 (0.37-0.43)	14	22
02254	0.73 (0.69-0.76)	0.72 (0.68-0.75)	0.71 (0.68-0.75)	0.62 (0.59-0.65)	0.60 (0.57-0.63)	0.59 (0.56-0.63)	15	19
00927	0.63 (0.60-0.66)	0.62 (0.59-0.64)	0.62 (0.59-0.64)	0.50 (0.48-0.52)	0.49 (0.46-0.51)	0.48 (0.46-0.51)	21	24
01602	0.76 (0.71-0.81)	0.74 (0.69-0.79)	0.72 (0.67-0.77)	0.61 (0.57-0.65)	0.59 (0.55-0.64)	0.58 (0.54-0.62)	20	24
03140	0.57 (0.51-0.62)	0.55 (0.50-0.60)	0.56 (0.51-0.61)	0.44 (0.40-0.47)	0.41 (0.38-0.45)	0.38 (0.35-0.41)	23	33
04964	1.75 (1.66-1.83)	1.75 (1.67-1.84)	1.75 (1.66-1.84)	1.74 (1.65-1.82)	1.73 (1.65-1.82)	1.73 (1.65-1.82)	1	1
04936	1.02 (0.98-1.05)	1.00 (0.97-1.04)	1.00 (0.96-1.03)	1.00 (0.97-1.04)	0.98 (0.95-1.02)	0.98 (0.94-1.02)	2	4

	no binning			binning by 1/4 pixel			improvement(%)	
	a	b	c	A	B	C	a->A	a->C
02228	0.51 (0.47-0.54)	0.48 (0.44-0.53)	0.47 (0.43-0.52)	0.43 (0.40-0.46)	0.40 (0.37-0.43)	0.39 (0.37-0.42)	16	24
02254	0.73 (0.69-0.76)	0.72 (0.68-0.75)	0.71 (0.68-0.75)	0.57 (0.54-0.60)	0.56 (0.54-0.59)	0.56 (0.54-0.59)	22	23
00927	0.63 (0.60-0.66)	0.62 (0.59-0.64)	0.62 (0.59-0.64)	0.45 (0.43-0.47)	0.43 (0.41-0.45)	0.42 (0.40-0.44)	29	33
01602	0.76 (0.71-0.81)	0.74 (0.69-0.79)	0.72 (0.67-0.77)	0.59 (0.56-0.63)	0.54 (0.51-0.57)	0.51 (0.48-0.55)	22	33
03140	0.57 (0.51-0.62)	0.55 (0.50-0.60)	0.56 (0.51-0.61)	0.39 (0.36-0.43)	0.40 (0.37-0.43)	0.30 (0.28-0.33)	32	47
04964	1.75 (1.66-1.83)	1.75 (1.67-1.84)	1.75 (1.66-1.84)	1.74 (1.66-1.83)	1.73 (1.65-1.82)	1.74 (1.65-1.82)	1	1
04936	1.02 (0.98-1.05)	1.00 (0.97-1.04)	1.00 (0.96-1.03)	1.03 (0.99-1.06)	0.99 (0.95-1.02)	0.98 (0.95-1.02)	0	4

a and A: pipeline products
b and B: pixel randomization off
c and C: sub-pixel algorithm applied

*** Applying sub-pixel binning (1/4), the source size is reduced by 19-24%.**
*** Removing pixel randomization and applying the sub-pixel algorithm, the source size is further reduced by another 6-8%**
*** However, no improvement for off-axis sources**

Test 2: Improvement in detection of faint sources embedded in diffuse emission

With the improved resolution, we detect ~20% more faint sources when embedded on the extended, diffuse emission in a crowded field. To check whether the new sources are real or suprious, we compare sources detected in shallow and deep images.

We assume that the real (false) source which are newly found in the shallow image would (not) be detected in the deep image. Because some point sources (LMXBs) in elliptical galaxies are variable, the false source rate is actually an upper limit. To lessen the affect of variable sources, we cut a deep observation (90-110 ks) into smaller pieces (10ks and 20ks), instead of merging multiple observations taken in different observation times.

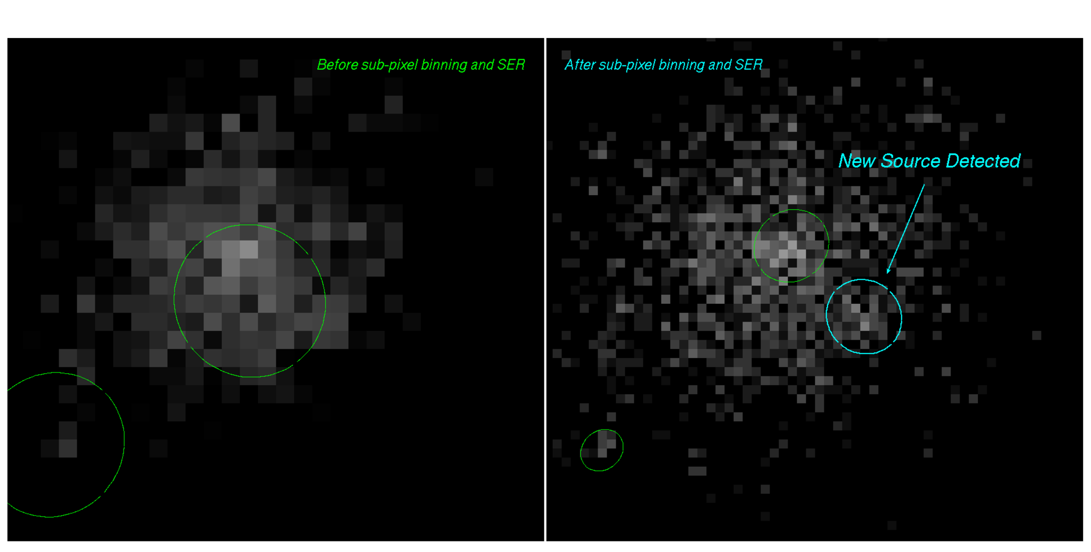

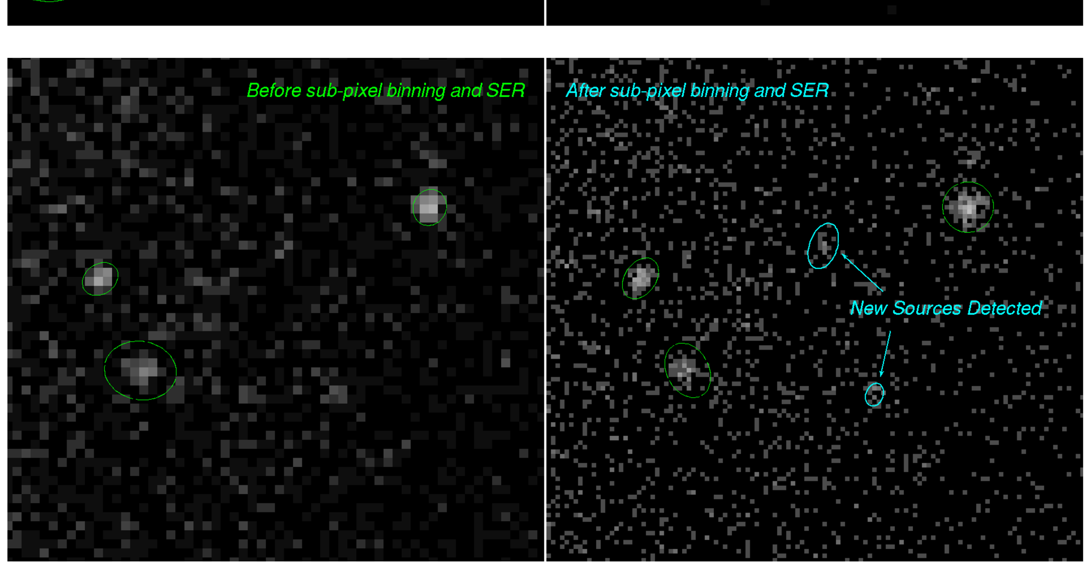

In n-m,
n= number of new sources confirmed in the deeper image.
m= number of new sources not confirmed in the deeper image.

		sub-pixel binning				binning + sub-pixel algorithm			
	O	A	B	C	D	A	B	C	D
NGC 3379 obsid=7073 (87 ks)									
1 10ks	32	0-0	4-0	0-0	4-0	2-0	8-1	2-0	7-0
2 10ks	34	2-0	4-1	2-0	2-0	2-1	4-0	2-0	3-0
3 10ks	30	0-0	2-0	0-0	2-0	0-0	3-1	0-0	2-0
4 20ks	52	2-0	4-3	2-0	3-2	4-1	6-3	4-0	6-1
5 20ks	48	1-0	3-4	1-0	2-0	2-1	4-4	2-1	4-0
6 20ks	44	2-2	6-4	2-2	5-1	3-1	8-2	2-2	8-0
Subtotal	240	7-2	23-12	7-2	18-3	13-4	33-11	**12-3**	**30-1**
NGC 4278 obsid=7081 (114 ks)									
1 10ks	40	2-0	8-2	1-0	3-1	5-0	15-0	5-0	10-0
2 10ks	40	4-0	6-1	4-0	5-0	4-1	14-2	4-1	11-1
3 10ks	38	3-0	3-1	2-0	1-1	3-0	11-0	3-0	5-0
4 20ks	62	2-0	13-6	3-0	9-0	3-0	16-11	3-0	13-3
5 20ks	61	5-1	8-5	5-1	3-0	8-1	22-6	8-0	20-1
6 20ks	65	2-1	4-0	2-1	1-0	5-1	14-4	5-1	11-0
Subtotal	306	18-2	42-15	16-2	21-3	28-3	92-23	**27-2**	**70-5**
Total	**546**	**25-4**	**65-27**	**23-4**	**39-6**	**41-7**	**125-34**	**39-5**	**100-6**

O. number of sources from the pipeline image binned by ACIS pixel (0.492")
A. number of lost sources (i.e., detected in the raw image, but not in the sub-pix image)
B. number of new sources (i.e., detected in the sub-pix image, but not in the raw image)
C. same as A, but exclude those sources with 0 size by wavdetect (r_major=r_minor=0)
D. same as B, but exclude those sources with 0 size by wavdetect (r_major=r_minor=0)

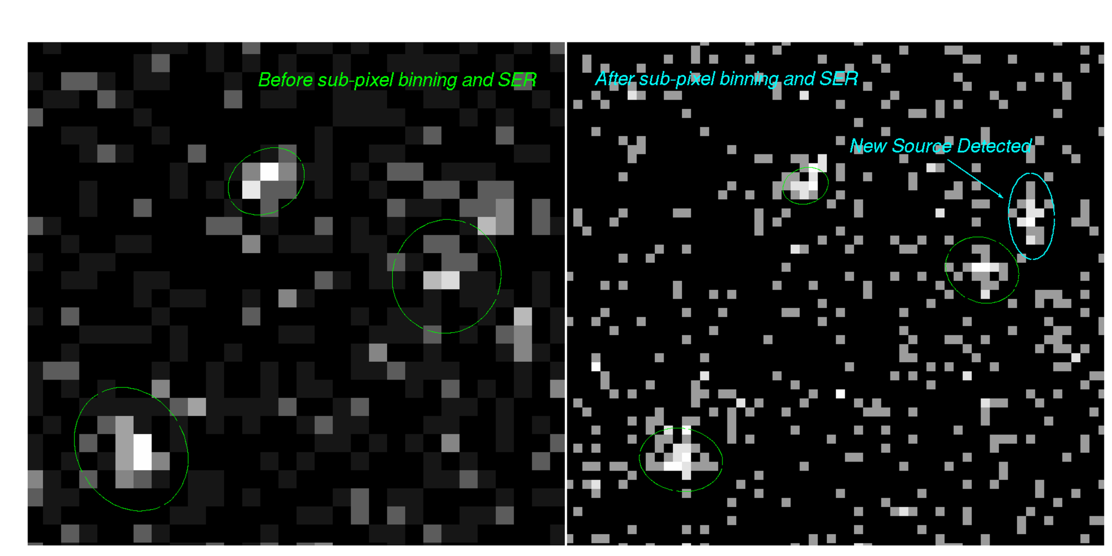

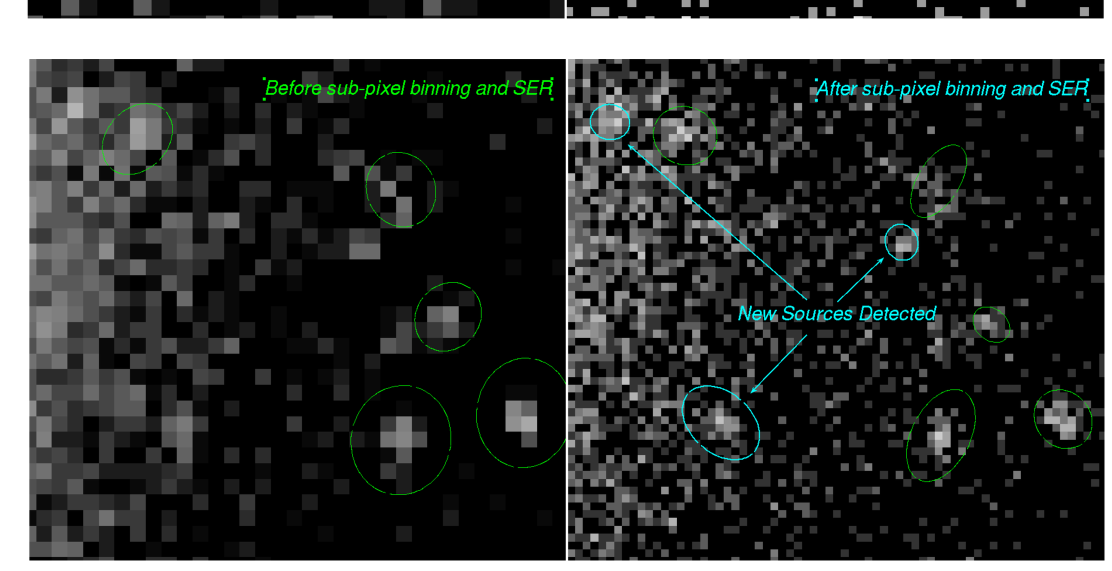

Chandra Re-processing

The new sub-pixel algorith will be implemented in the next major reprocessing which is expected to start within 2011.

~20% more sources detected with false source rate of ~10%

- After binning by 1/2 pixel the fraction of new sources is 8-9% (21/240, 24/306) of which 13-14% (3/21, 3/24) may be false, i.e., not detected in the deeper image.
- After applying the algorithm and binning by 1/2 pixel, the fraction of new sources is 13-25% (31/240, 75/306) of which 3-7% (1/31, 5/75) may be false.
- 6-9% (15/240, 29/306) of original sources are lost. 7-26% of them (3/15, 2/29) may be false, i.e., not in the deeper image. - original detections still necessary.
- However, there is no improvement when the background and diffuse emissions are low. e.g., a similar test with CDF-S data found that most new sources are false.

No Grid Structure by Aliasing

In the previous Chandra processing, the pixel randonmization was applied to remove the grid structure by an aliasing effect and to improve the source position. We confirmed that the new sub-pixel algorithm (without pixel randomization) does **not** introduce a grid structure as long as the dither was on during the observation and does not worsen the positional accuracy of detected sources.